

# Dynamics of earth dams under shock impacts

Mirziyod Mirsaidov<sup>1\*</sup>, Elyor Toshmatov<sup>1,2</sup>, and Bakhtiyor Urinov<sup>1</sup>

<sup>1</sup>National Research University-Tashkent Institute of Irrigation and Agricultural Mechanization Engineers, Tashkent, Uzbekistan

<sup>2</sup>Institute of Mechanics and Seismic Stability of Structures of the Academy of Sciences of the Republic of Uzbekistan, Tashkent, Uzbekistan

**Abstract.** The article provides a detailed analysis of well-known studies, which allow considering the work of the structure together with the base under dynamic influences, adequate replacement of an infinite base with a finite one using non-reflecting conditions on the boundary of the finite region, well-known methods for assessing the behavior of a structure under impact. A mathematical model, method, and algorithm were developed to evaluate the dynamic behavior of earth dams together with the base under shock impact using non-reflective conditions based on Rayleigh waves on the boundaries of the finite area of the base. To simulate a dynamic process, the principle of virtual displacements is used, taking into account the viscoelastic properties of the material. The solution to the problem is conducted by the finite element method and the Newmark method. The dynamic behavior of earth dams, together with the base, is studied, considering non-reflecting conditions under explosive impacts that arise not far from the structure. It was established that during the period of wave travel, a non-synchronous movement of individual parts of the dam occurs, damped due to the wave entrainment of energy and the viscoelastic properties of the material. It was revealed that the maximum principal stresses  $\sigma_1$  occur in the lower part of the upper slope of the dam and gradually spread along the entire dam; the maximum principal stresses  $\sigma_2$  are reached near the foot of the dam and, as the wave propagates, they move along the base directly behind the wavefront; the maximum values of shear stress  $\sigma_{12}$  are reached on the surface of the upper slope, first at the foot of the dam, then over the entire surface of the slope.

## 1 Introduction

To evaluate the dynamic behavior of an earth dam under impacts occurring not far from the structure, it is necessary to consider it with the base of the structure. At that, for a single system of construction with a base, it becomes more difficult to solve the dynamic problem due to the infinite dimensions of the base. Therefore, for an adequate description of the dynamic processes in the structure-base system, selecting an equivalent model reflecting the real processes occurring in the base of such a system is necessary. In this article, for such a model, it is proposed to use a finite base model cut out of an infinite base, placing on fictitious (artificial) boundaries of the finite area that do not reflect the boundary conditions

---

\* Corresponding author: [theormir@mail.ru](mailto:theormir@mail.ru)

based on the Rayleigh wave, which ensured the energy entrainment from the structure to infinity [1-3]. Therefore, this condition is often called wave entrainment of energy (or wave dissipation) since it ensures the entrainment of energy in the form of a wave from the structure to infinity. To avoid parasitic resonant phenomena, when solving specific dynamic problems, the viscoelastic properties of soil are taken into account; they provide internal dissipation both in structures and in bases [3].

There are several works that propose the use of non-reflecting conditions on the boundary of a finite region for the equivalent replacement of an infinite base with a finite one:

- the study in [4] presents a comprehensive accuracy assessment of the calculation procedure related to the analysis of the response history of the dam, modeled as a system of finite elements, including the interaction of the dam with water and base. It is noted that the level of accuracy is achieved in the calculation procedure by considering the dam-base interaction and water absorption of the reservoir bottom on the dynamics of the system;

- in [5], a direct formulation of the finite element method for the non-linear analysis of interacting dam-water-base systems during earthquakes is presented. When calculating the system, the absorption of a viscous damper is determined on the boundaries of a truncated area cut out from a semi-infinite fluid and basement rock. The effective earthquake forces are defined at these boundaries. The frequency response functions and transient responses of the idealized dam-water-base system are numerically calculated, and the results obtained are compared with the results obtained by the substructure method;

- in [6], a simplified direct finite element (FE) method was used for non-linear analysis of the response history of semi-infinite dam-water-base systems. The analysis uses a standard absorbing viscous damper on finite region boundaries to simulate semi-infinite base and fluid regions. The seismic input as the effective earthquake forces determined from the control motion was defined on the base surface and at these boundaries;

- in [7], the model of the global system of the Koina dam was created using the ABAQUS software, taking into account the interaction of the dam, reservoir, and base. Uncoupled and coupled models were compared concerning the horizontal displacement of the dam crest and the differential subsidence of the dam base on the clayey bed. Uncoupled model results determined overestimated predicted stability and damage detection in the dam. The modulus of elasticity of the clayey base was the decisive parameter determining the change in the differential subsidence of the dam base. When modeling the operation of the system, viscous dampers were used at the boundary of the clayey base;

- in [8], when assessing the dynamic behavior of specific earth dams, the issue of the need to exclude waves reflected from the boundary of the finite area of the base was discussed; special conditions were used when solving specific problems;

- in [9,10], using the condition that ensures the transmission of energy through the boundaries of the finite region of the base, three-dimensional non-linear problems of the structure dynamics were solved. The effectiveness of this condition was verified by comparison with the usual condition of a viscous boundary on the boundaries of a finite base region.

- in [11], when solving dynamic problems by numerical simulation, an artificial boundary condition was used, which reduces wave reflections from the boundaries of the model. The absorbing characteristics of such a condition were evaluated using theoretical analysis and numerical experiments.

- an approximate local operator was constructed in [12] for harmonic elastic waves. Exact operators were obtained using Fourier analysis for an elastic half-space. The approach's effectiveness was studied for various geometries of an obstacle at high frequencies.

- in [13], an absorbing boundary condition for an acoustic wave was developed using

the method without a grid. When modeling the acoustic wave propagation by numerical method, artificial reflections from the model's edges should be avoided. Numerical experiments showed that the proposed method could provide a good effect in suppressing reflections from artificial model boundaries.

-the study in [14] considers the seismic analysis of the dam-base system using the finite element method. To simulate a semi-infinite subgrade, a local non-reflective cone-type boundary condition was used. The results show the superiority of the proposed condition in absorbing the reflection of false waves over the traditional viscous boundary conditions.

The fundamental work [15] analyzes published articles that use artificial boundary conditions on the boundary of a finite region and the results obtained in these articles. It also considers the problem of setting correct boundary conditions on the artificial boundaries of the computational domain, mathematical justification, analysis, and efficiency of using such conditions in solving specific problems.

Along with this, there are publications [16-26] in which the dynamic behavior and wave phenomenon in various systems are studied, taking into account their design features and various properties of their material.

Here is a review of only some of the works devoted to the problem of studying the dynamic behavior of the structure-base system using artificial non-reflective conditions on the boundary of the finite region of the base, which ensure the energy entrainment.

Summing up this review, it should be noted that the problem of assessing the dynamic behavior of nonhomogeneous structures, together with the base, when solving dynamic problems under shock or explosive loads that arise near the structure, considering the energy entrainment from the structure to infinity and the dissipative properties of both the structure itself and its base are far from the final solution and present an urgent task.

This work aims to develop a mathematical model, methods, and algorithms for assessing the dynamic behavior of a structure under explosive loads that appear near the structure and act on the base and to study the dynamics of specific structures under various impacts.

Consider a plane inhomogeneous system consisting of an earth dam and a base (Fig. 1) located on an infinite deformable half-space (i.e., on a ground base). To simulate the dynamic processes occurring in the system under consideration under the impact, the finite region of volume  $V_5$  is cut with boundaries  $\Sigma_1^-, \Sigma_1^+, \Sigma_2^+$ . Half-space material is assumed to be elastic or viscoelastic.

The structure is inhomogeneous and occupies volume  $V_1 + V_2 + V_3$ , the material of different parts of the system can be elastic and viscoelastic, and the physical properties of their components differ. The base occupies volume  $V_4$  and is elastic. At the boundary between the system elements ( $V_1, V_2, V_3, V_4, V_5$ ), there are continuous displacements, normal and tangential to the boundary surface stress components. A shock (explosive) load  $\vec{p}(t)$  acts on the system under consideration (Fig. 1) on the site  $\Sigma_p$ . The structure itself is massive, so the mass forces  $\vec{f}$  are also considered in calculations.

The task is to determine the dynamic behavior of the structure (Fig. 1) under the influence of shock (explosive) loads  $\vec{p}(t)$ .

The problems under consideration are posed for a finite region (Fig. 1) of volume  $V = V_1 + V_2 + V_3 + V_4 + V_5$ . Here  $V_5$  is the volume of the region cut out from the half-space and bounded by surfaces.

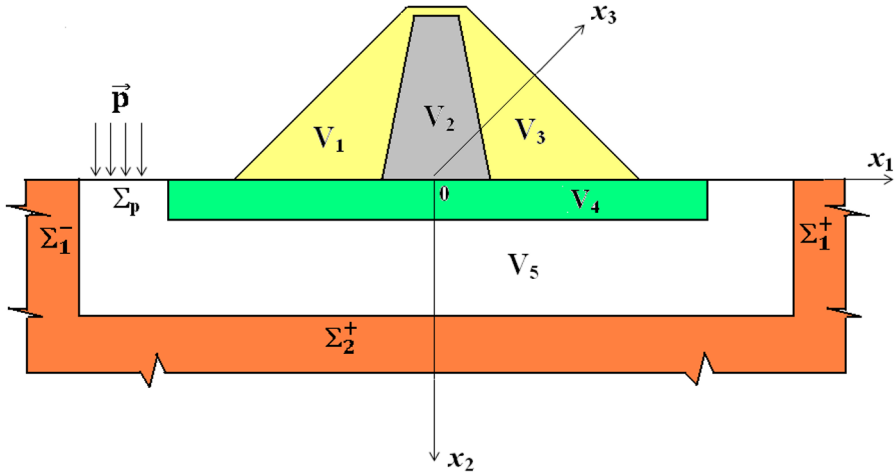


**Fig. 1.** Calculation model of earth dam, bearing shock load at base.

To describe the dynamic processes occurring in the system (Figure 1.), the principle of virtual displacements is used, according to which the sum of the work of all active forces, including inertia forces, on virtual displacements is zero, i.e.:

$$\begin{aligned} \delta A = & - \int_V \sigma_{ij} \delta \epsilon_{ij} dV - \int_V \rho_n \ddot{u} \delta \bar{u} dV + \int_{\Sigma_1^- + \Sigma_1^+ + \Sigma_2^+} \sigma_{ij} \nu_j \delta \bar{u} d\Sigma + \\ & + \int_{V_1 + V_2 + V_3 + V_4} \vec{f} \delta \bar{u} dV + \int_{\Sigma_p} \vec{p} \delta \bar{u} d\Sigma = 0 \end{aligned} \tag{1}$$

Then, to describe the physical properties of the body, the relations between the components of stress  $\sigma_{ij}$  and strain  $\epsilon_{ij}$  tensors of the form [27] are used:

$$\sigma_{ij} = \tilde{\lambda}_n \epsilon_{kk} \delta_{ij} + 2\tilde{\mu}_n \epsilon_{ij} \tag{2}$$

In the case when the material of the  $n$ -th element of the system is elastic, the quantities  $\tilde{\lambda}_n$  and  $\tilde{\mu}_n$  are the Lamé constants; if the material has viscoelastic properties, then  $\tilde{\lambda}_n$  and  $\tilde{\mu}_n$  are the Volterra integral operators and have the form [27]:

$$\left. \begin{aligned} \tilde{\lambda}_n \varphi &= \lambda_n \left[ \varphi(t) - \int_0^t \Gamma \lambda_n(t-\tau) \varphi(\tau) d\tau \right] \\ \tilde{\mu}_n \varphi &= \mu_n \left[ \varphi(t) - \int_0^t \Gamma \mu_n(t-\tau) \varphi(\tau) d\tau \right] \end{aligned} \right\} \tag{3}$$

- the Cauchy relations are used that relate the components of the strain tensor  $\epsilon_{ij}$  to the components of the displacement vector  $\vec{u}$  [27]:

$$\varepsilon_{ij} = \frac{1}{2} \left( \frac{\partial u_i}{\partial x_j} + \frac{\partial u_j}{\partial x_i} \right), i=1,2 \quad (4)$$

non-reflective conditions are used at the boundary of the finite region of the base [1-3].

$$\begin{aligned} \bar{x} \in \Sigma_1^\pm: \quad & \frac{\partial u_i}{\partial x_1} \pm \frac{1}{\bar{c}_R} \frac{\partial u_i}{\partial t} = 0, \\ \bar{x} \in \Sigma_2^\pm: \quad & u_i = 0, i=1,2 \end{aligned} \quad (5)$$

and initial conditions are set at  $t = 0$ :

$$\bar{x} \in V: \bar{u}(\bar{x}, 0) = \bar{\psi}_2(\bar{x}); \dot{\bar{u}}(\bar{x}, 0) = \bar{\psi}_3(\bar{x}). \quad (6)$$

Condition (5) ensures energy transfer from the structure to infinity in the form of a Rayleigh wave through the boundaries of the finite region  $V_5$ .

Here:  $\bar{u}$ ,  $\varepsilon_{ij}$ ,  $\sigma_{ij}$  are the components of the displacement vector  $\bar{u} = \{u_1, u_2\}$ , strain and stress tensors, respectively;  $\delta \bar{u}$ ,  $\delta \varepsilon_{ij}$  are the isochronous variations of displacements and strains;  $\rho_n$  is the density of the material of the  $n$ -th element of the system;  $\bar{f}$  is the vector of mass forces;  $\bar{p}$  is the vector of shock (explosive) loads;  $\lambda_n, \mu_n$  are the Lamé constants;  $\Gamma_{\lambda_n}, \Gamma_{\mu_n}$  are the relaxation kernels;  $\varphi(t)$  is an arbitrary time function;  $\bar{\psi}_2, \bar{\psi}_3$  are the given coordinate functions;  $V_j$  is the direction cosines of the outer normal;  $\bar{c}_R$  is the Rayleigh wave propagation in a half-space (considering viscoelastic properties of the base material, these quantities are complex quantities);  $n = 1, 2, 3, 4, 5$  are the numbers of the system elements;  $\bar{x} = \{x_1, x_2\}$ ;  $i, j = 1, 2$ .

Now, the variational problem of unsteady-state forced vibrations of the system under consideration (Fig. 1) is reduced to determining the displacement  $\bar{u}(\bar{x}, t)$  and stress  $\sigma_{ij}(\bar{x}, t)$  fields in the structure under the mass forces  $\bar{f}$  and shock impacts  $\bar{p}(t)$  satisfying equations (1) - (4) taking into account (5) and condition (6) at any virtual displacement  $\delta \bar{u}$ .

## 2 Methods and algorithms

The problem under consideration is solved [28] by the finite element method (FEM) with the partition of region  $V$  into various types of finite elements. In solving specific problems, the division of region  $V$  (Figure 1.) into finite elements is performed, taking into account the design features and physico-mechanical properties of the material of different system parts.

Under short-term dynamic impacts (explosive ones), the unsteady-state forced vibrations arise in the system (Figure 1), the study of which allows us to determine the maximum values of displacements and stresses of the structure during the entire process of impact and to identify the most stressed sections in the system, taking into account various

inhomogeneous parameters of the material and design features of the structure.

The problem of unsteady-state forced vibrations of a system (Figure. 1) using the FEM procedure is reduced to solving a system of linear integro-differential equations

$$[M]\{\ddot{u}(t)\} + [C]\{\dot{u}(t)\} + [K]\{u(t)\} = \{F\} + \{f(t)\} + \int_0^t \Gamma(t-\tau)[K]\{u(\tau)\}d\tau \quad (7)$$

With initial conditions

$$\{u(0)\} = \{u_0\}, \quad \{\dot{u}(0)\} = \{v_0\} \quad (8)$$

Here  $[M]$ ,  $[K]$  are the matrices of mass and rigidity of the system;  $[C]$  is the matrix that takes into account the wave entrainment of energy;  $\{u(t)\}$  is the vector of the sought amplitudes of displacements;  $\{f(t)\}$  is the vector of dynamic load from explosive impacts;  $\Gamma$  is the relaxation kernel;  $\{F\}$  is the total vector of static loads (mass forces, the hydrostatic pressure of water, etc.).

The system of integro-differential equations (7) is solved under the initial conditions (8) by the Newmark method [28].

For this, the system of equations (7) under the initial conditions (8), at each time step  $\Delta t$ , is reduced to solving the algebraic system of equations

$$[A]\{u_{i+1}\} = \{R_{i+1}\}, \quad (9)$$

Where

$$[A] = [K] + \frac{1}{\alpha\Delta t^2}[M] + \frac{\beta}{\alpha\Delta t}[C], \quad (10)$$

in this case, the right-hand side  $\{R_{i+1}\}$  of equation (9) is determined using the expression

$$\begin{aligned} \{R_{i+1}\} = & \langle F \rangle + \{f(t_{i+1})\} + [M]\left\{\frac{1}{\alpha\Delta t^2}\{u_i\} + \frac{1}{\alpha\Delta t}\{\dot{u}_i\} + \left(\frac{1}{2\alpha} - 1\right)\{\ddot{u}_i\}\right\} + \\ & + [C]\left\{\frac{\beta}{\alpha\Delta t}\{u_i\} + \left(\frac{\beta}{\alpha} - 1\right)\{\dot{u}_i\} + \frac{\Delta t}{2}\left(\frac{\beta}{\alpha} - 2\right)\{\ddot{u}_i\}\right\} + \\ & + \{W_{i+1}\}, \end{aligned} \quad (11)$$

$$\{W_{i+1}\} = \int_0^{t_{i+1}} \Gamma(t-\tau)[K]\{u_i\}d\tau \quad (12)$$

To solve the obtained system of algebraic equations (9), it is necessary to specify at the initial moment ( $t = 0$ ) the values of displacements  $\{u_0\}$ , velocity  $\{\dot{u}_0\}$ , and accelerations  $\{\ddot{u}_0\}$ . Normally  $\{\ddot{u}_0\} = 0$  is set.

The Newmark method is unconditionally stable if  $\beta \geq 0.5$ ,  $\alpha \geq 0,25(\beta + 0,5)^2$ . Thus, an algorithm that implements the Newmark method for solving the system of integro-differential equations (7) with the initial condition (8) has the following form:

1. The initial values  $\{u_0\}, \{\dot{u}_0\}, \{\ddot{u}_0\} = 0$  are set.
2. A system of algebraic equations (9) is formed with the right-hand side (11) - (12) describing elastic and viscous properties of the material of the system.
3. The resulting algebraic system of equation (9) is solved by the Gaussian method or the square root method.

A feature of the algorithm is that the integrals entering expression (12) of the vector  $\{W_{i+1}\}$  are calculated from the beginning of the process. In contrast, the integrals at each step are determined in the range from  $t_i$  to  $t_{i+1}$ . Moreover, the total value of  $\{W_{i+1}\}$  at time  $t_{i+1}$  is obtained by summing the value  $\{W_i\}$  saved in the previous step with the integral obtained at the last stage with the integration limits from  $t_i$  to  $t_{i+1}$ .

### 3 Results and discussion

To verify the reliability of the developed algorithms and calculation program, the Newmark method was used to solve integro-differential equations [29]

$$\dot{y}(t) + \omega^2 \left[ y(t) - \int_0^t \Gamma(t - \tau) y(\tau) d\tau \right] = -f(t) \tag{13}$$

At initial conditions

$$y(0) = 1, \dot{y}(0) = -\beta \tag{14}$$

And initial data, i.e., A.R.Rzhanitsyn kernel [30]

$$\Gamma(t) = Ae^{-\beta t} \cdot t^{\alpha-1} \tag{15}$$

And right-hand side with initial data

$$f(t) = \left[ \beta^2 + \omega^2 - \frac{A\omega^2 t^\alpha}{\alpha} \right] e^{-\beta t}, A = 0.01; \alpha = 0.25; \omega = 2\pi; \rho = 0.01$$

The system of integro-differential equations (13) under the initial conditions (14) has an exact solution  $y = e^{-\beta t}$ .

Table 1 compares solution results obtained with the developed algorithm at various values of  $t$  with exact solutions of equations (13) under initial conditions (14).

**Table 1.** Solution of integro-differential equations

Solution of integro-differential equations. Time, $t$ , s	0.4	1.2	2.0	4.0	8.0	12.0	16.0	20.0	24.0	28.0
The solution obtained by the Newmark method	0.97	0.92	0.88	0.80	0.65	0.53	0.43	0.36	0.29	0.24
Exact solution	0.98	0.94	0.90	0.81	0.67	0.54	0.44	0.36	0.30	0.24

A comparison of results presented in Table 1 shows that using the developed algorithm based on the Newmark method, the solution of integro-differential equations can be obtained with the desired accuracy.

Using the above model and algorithm, the dynamic behavior of an inhomogeneous system (Fig. 1) was investigated in a plane statement. In this case, the ground base was considered an elastic one, and the structure was viscoelastic. The shock impact was taken as an external load, changing according to the following law:

$$\bar{x} \in \Sigma_p: P(t) = \begin{cases} 100000 & t = 0 \\ -250000 t + 100000 & \text{at } 0 \leq t < 0.4 \text{ sek} \\ 0 & t \geq 0.4 \text{ sek} \end{cases} \quad (16)$$

The load  $P(t)$  in kN is also plane and applied at a distance of 25 m from the dam foot on the base surface, i.e., at the site  $\Sigma_p$  (Fig. 1). It is necessary to determine the fields of displacements and stresses in the dam body at various points in time arising under shock (explosive) loads (16).

In calculations, it was accepted:

-for the dam: height  $H = 168.0$  m, the ratio of the upstream and downstream slopes  $m_1 = m_2 = 2.2$ ; crest width  $b = 10.0$  m; material properties: elastic modulus  $E = 3000.0$  MPa; Poisson's ratio  $\nu = 0.3$ ; specific gravity of soil  $\gamma = 2.2$  tf/m<sup>3</sup>. In this case, A.R. Rzhanitsyn kernel was used (15) to consider soil's viscoelastic properties. The parameters  $A, \alpha, \beta$  of the kernel (15) for various soils were determined in [31] (from experimental data using the technique [27]) and taken in the form:  $A = 0.0146$ ;  $\alpha = 0.2$ ;  $\beta = 0.0000057$ .

-for the ground base of the structure, material properties are elastic modulus  $E = 3600.0$  MPa; Poisson's ratio  $\nu = 0.3$ ; specific gravity of soil  $\gamma = 2.8$  tf/m<sup>3</sup>.

The solution to this problem at the set parameters revealed that the load  $P(t)$  arising from the impact creates a non-uniform wave field of displacements in the dam body. The beginning of motion of each point of the structure corresponds to the time of the wavefront approach to it, determined by the distance of the point from the load application point and the wave propagation in soil.

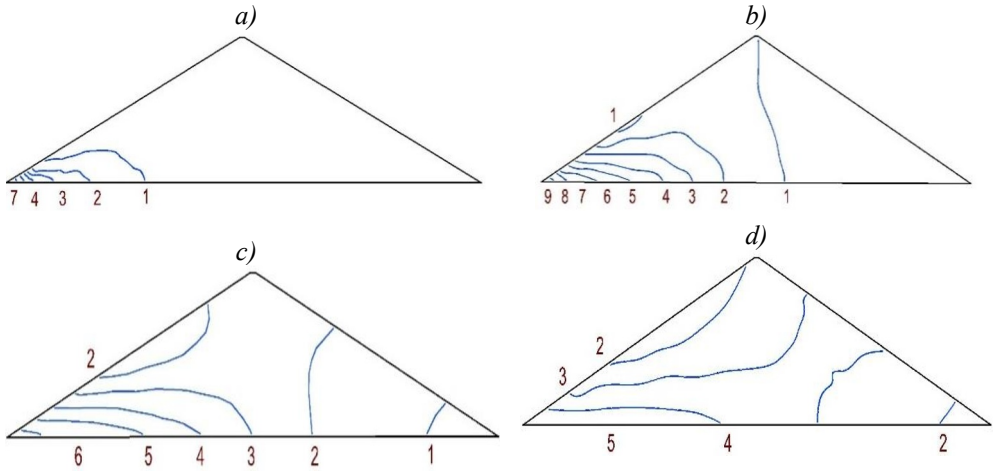
The results show that various structure points do not enter into motion simultaneously. The beginning of each point motion corresponds to the time of the blast wave front approach to it. This time is uniquely determined by the distance of the point from the explosion source and the wave propagation in the soil.

Figure 2 shows the isolines of the horizontal displacement distribution in the dam cross-section at different points in time. The wave generated by explosive load, located relative to the dam foot, passing along the ground base first causes a displacement in the foot of the upper slope (Figure 2a) and eventually covers more distant areas of the structure (Figure 2. c, d). In this case, the lower region of the upstream slope, bounded by isoline "1", remains stationary due to wave diffraction at the base-slope junction. The isoline with the same index on the lower slope (Figure 2b) corresponds to the position of the wavefront, in front of which there is an undisturbed (at  $t = 0.46$  sec) area of the dam (the right side of the figure). At subsequent points in time, the disturbance from the explosive load  $P(t)$  completely covers the dam body, and the horizontal displacement distribution in it is represented by isolines in Figures 2a-d. After the wave propagation, the strained state of the dam gradually stabilizes.

The values of horizontal displacements on isolines (Figure 2.) increase at an equal interval of  $0.005$  m beginning from  $0.0$  m - isoline "1". The maximum displacements are  $0.042$  m and are observed in the area bounded by the line with the index "9"; the



displacement in the line is 4 cm.



**Fig. 2.** Isolines of horizontal displacements (m) distribution in the dam cross section at different points in time  $t$ : (a) 0.2 s, (b) 0.32 s, (c) - 0.52s, (d) - 0.60s

The stress state of the dam, represented by the principal stresses ( $\sigma_1$ ) at various points in time: at the beginning, in the middle, and at the end of the process, is shown in Fig. 3. The stress dimension is MPa.

At the initial time of the process, the lower part of the dam upstream slope is deformed, and a tension zone with positive stresses  $\sigma_1$  appears (line "2" in Fig. 3, a), which spreads up the slope as the wave propagates (Fig. 3b, c ) and to the entire internal region of the dam (Fig. 3c, d). The magnitude of the stresses  $\sigma_1$  on the isolines (Fig. 3) varies with the same step of 0.05 MPa: from 0.0 MPa - on the line "1" to 0.3 MPa - on the line "6".

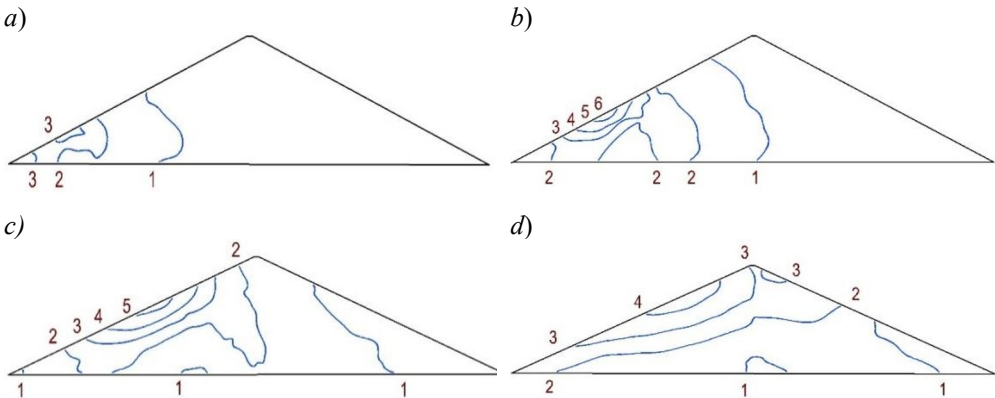


**Fig. 3.** Isolines of distribution of principal stresses  $\sigma_1$  in the dam cross section at different points in time  $t$ : (a) 0.2s, (b) 0.32s, (c) 0.52s, and (d) 0.60s

The maximum tangential stresses ( $\sigma_{12}$ ) arise on the surface of the upstream slope (Figure 4.): first, at its foot and then along the entire height; this is fraught with the possibility of a landslide on the slope (Figure 4.).

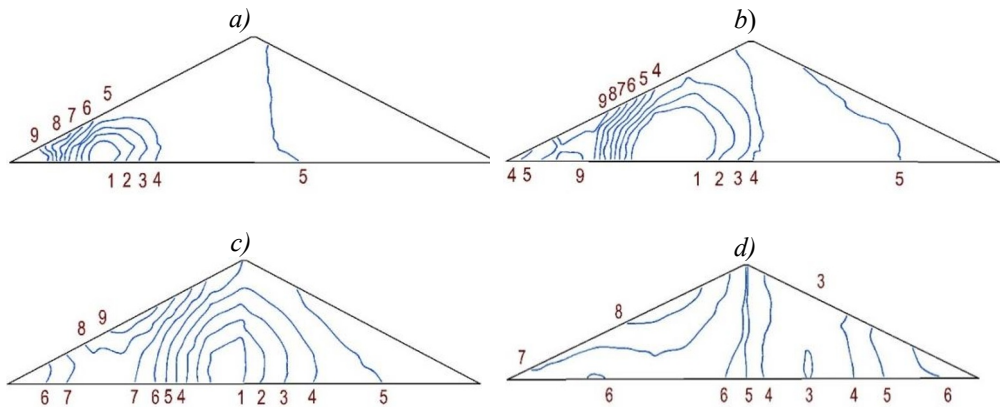


**Fig. 4.** Isolines of distribution of tangential stresses  $\sigma_{12}$  in the dam cross-section at different points in t: (a) 0.2s, (b) 0.32s, (c) 0.52s, and (d) 0.60s.

The values of tangential stresses  $\sigma_{12}$  at the isolines (Figure 4.) vary with a step of  $\pm 0.025$  MPa from 0.0 MPa on the line "5" to  $\pm 0.1$  MPa on the lines "1" and "9".

## 4 Conclusion

1. A mathematical model, method, and algorithm were developed for assessing the dynamic behavior of a structure together with the foundation, taking into account internal dissipation based on a linear hereditary model of viscoelasticity and wave entrainment of energy using non-reflective conditions at the boundary of the finite area of the ground base.

2. To assess the method's reliability, a test problem was solved, and the results were compared with the exact solution of integro-differential equations.

3. The study of the dynamic behavior of the structure together with the base under shock (explosive) impacts using wave entrainment of energy through the boundary of the finite area of the base showed that:

- maximum principal stresses  $\sigma_1$  arising in the lower part of the upper the slope gradually spread to the entire slope and the central area of the dam;
- maximum principal stresses  $\sigma_2$  are reached near the foot of the dam and as the waves propagate, they move along the base immediately behind the wavefront;
- maximum values of tangential stresses  $\sigma_{12}$  are achieved at the surface of the upper slope, first at the foot of the dam, then along the entire slope's surface. There are no shear stresses in the center of the dam;
- during the period of wave passage in the dam, the symmetrical stress distribution is disturbed;
- there is a non-synchronous movement of the parts of the dam, damped due to the wave entrainment of energy (wave dissipation) and viscoelastic properties (internal dissipation) of the material in the system under consideration.

## References

1. Mirsaidov M. M., Troyanovsky I. E. The wave problem of the earthquake resistance of a structure under the Rayleigh wave propagation in elastic half-space. of AS RUz, ser., No. 5, Tech. Sci. – Tashkent, Pp. 48-51, 1980.
2. Mirsaidov M.M., Sultanov T.Z., Rumi D.F. An assessment of dynamic behavior of the system "structure - Foundation" with account of wave removal of energy. Magazine of Civil Engineering, 39(4), Pp. 94-105, 2013.
3. Mirsaidov M.M., Troyanovsky E.I. Dynamics of inhomogeneous systems with allowance for internal dissipation and wave entrainment of energy. Tashkent: Fan, P.108, 1990.
4. Arnkjell Løkke and Anil K. Chopra, M.ASCE. Response Spectrum Analysis of Concrete Gravity Dams Including Dam-Water-Foundation Interaction. Journal of Structural Engineering. 2015.
5. Løkke A., Chopra A. Direct finite element method for non-linear earthquake analysis of 3-dimensional semi-unbounded dam–water–foundation rock systems. Earthquake Engineering & Structural Dynamics.
6. Arnkjell Løkke, Anil K. Chopra. Direct finite element method for non-linear earthquake analysis of concrete dams: Simplification, modeling, and practical application. Earthquake Engineering & Structural Dynamics. 2019. doi: 10.1002/eqe.3150
7. Nazim Abdul Nariman, Tom Lahmer, Peyman Karampour, Uncertainty quantification of stability and damage detection parameters of coupled hydrodynamic-ground motion in concrete gravity dams. Front. Struct. Civ. Eng. Vol. 13. Issue (2). Pp. 303-323, 2019.
8. Meen-Wah Gui and Hsien-Te Chiu, Seismic response of Renyitan earth-fill dam. Journal of Geo Engineering. Vol. 4, № 2, Pp.41-50, 2009.
9. Nakamura N. Improvement of energy transmitting boundary for three-dimensional non-linear analysis. 16th World Conference on Earthquake Santiago Chile. Paper N° 1714 (16WCEE 2017).
10. Nakamura N. Three-dimensional energy transmitting boundary in the time domain. Front. Built Environ. 1:21, 2015. doi: 10.3389/fbuil.2015.00021
11. Y.Gao, H.Song, J.Zhang, Z.Yao Comparison of artificial absorbing boundaries for acoustic wave equation modeling // Exploration Geophysics. 48(1). Pp.76-93. (2015)
12. Chaillat S., Darbas M., Le Louër F. Approximate local Dirichlet-to-Neumann map for three-dimensional time-harmonic elastic waves. Computer Methods in Applied Mechanics and Engineering. Vol .297. 62-83, 2015.
13. Takekawa J., Mikada H. An absorbing boundary condition for acoustic-wave propagation using a mesh-free method.. 81(4) Pp.145-154, 2016.
14. Mandal A., Maity D. Finite Element Analysis of Dam-Foundation Coupled System Considering Cone-Type Local Non-Reflecting Boundary Condition. Journal of Earthquake Engineering.. 20, Issue 3, Pp.428-446, 2016.
15. Ilgamov M.A., Gilmanov A.N. Non-reflecting conditions at the boundaries of the computational domain. Moscow: Fizmatlit, P.240, 2003.
16. Ismailova S.I., Sultanov K.S. Non-linear deformation laws for composite threads in extension. Mechanics of Solids, 50(5) 578–590. 2015.
17. Sultanov K.S., Loginov P.V, Ismoilova S.I. Quasistaticity of the process of dynamic strain of soils. Magazine of Civil Engineering. No.1(85), pp.71–91, 2019.

18. Bakhodirov A.A., Ismailova S.I., Sultanov K.S. Dynamic deformation of the contact layer when there is shear interaction between a body and the soil. *Journal of Applied Mathematics and Mechanics*, 79(6) 587–595, 2015.
19. Mirsaidov M.M. et al., Assessment of dynamic behavior of earth dams taking into account large strains. *E3S Web of Conferences*. 97,05019. 2019.
20. Sultanov T.Z., Khodzhaev D.A., Mirsaidov M.M. The assessment of dynamic behavior of heterogeneous systems taking into account non-linear viscoelastic properties of soil. *Magazine of Civil Engineering*. 45(1), c. 80-89+117-118.
21. Usarov M., Mamatisaev G., Yarashov J., Toshmatov E. Non-stationary oscillations of a box-like structure of a building. *Journal of Physics: Conference Series*, 2020. <https://doi.org/10.1088/1742-6596/1425/1/012003>.
22. Yarashov J., Usarov M., Ayubov G. Study of longitudinal oscillations of a five-storey building on the basis of plate continuum model // *E3S Web of Conferences* 97, Form-2019, 04065, 2019.
23. Mirsaidov M.M., Sultanov T.Z., Sadullaev A. Determination of the stress-strain state of earth dams with account of elastic-plastic and moist properties of soil and large strains. *Magazine of Civil Engineering*. 40(5), Pp. 59-68.
24. Khodzhaev D.A., Abdikarimov R.A., Mirsaidov M.M., Dynamics of a physically non-linear viscoelastic cylindrical shell with a concentrated mass. *Magazine of Civil Engineering*. 91(7), Pp. 39–48, 2019. doi: 10.18720/MCE.91.4
25. Mirsaidov M.M., Boytemirov M., Yuldashev F. Estimation of the Vibration Waves Level at Different Distances. *Lecture Notes in Civil Engineering*, 170, Pp. 207–215, 2022.
26. Urazmukhamedova Z., Juraev D., Mirsaidov M.M. Assessment of stress state and dynamic characteristics of plane and spatial structure. *Journal of Physics: Conference Series*. 2070(1), 012156, 2021.
27. Koltunov M.A., Kravchuk A.S., Mayboroda V.P., *Applied mechanics of a deformable rigid body*. M.: Higher school. P. 349, 1983.
28. Bate K., Wilson E. *Numerical methods of analysis and FEM*. Moscow: Stroyizdat, P. 448, 1982.
29. Badalov F.B. *Methods for solving integral and integro-differential equations of the hereditary theory of viscoelasticity*. Tashkent: Mekhnat, P. 269, 1987.
30. Rzhantsyn A.R. *Creep theory*. Moscow: Stroyizdat, P. 416, 1968.
31. Mirsaidov M.M., Sultanov T.Z. Use of linear heredity theory of viscoelasticity for dynamic analysis of earthen structures. *Soil Mechanics and Foundation Engineering*. Vol. 49, Iss. 6, Pp. 250-256, 2013. doi: 10.1007/s11204-013-9198-8.